



Removal of microplastics and metals in biochar beds for stormwater treatment: Effects of prolonged drying and salinity on pollutant mobility

Downloaded from: <https://research.chalmers.se>, 2026-05-15 16:22 UTC

Citation for the original published paper (version of record):

Rullander, G., Herbert, R., Hvitt Strömvall, A. et al (2026). Removal of microplastics and metals in biochar beds for stormwater treatment: Effects of prolonged drying and salinity on pollutant mobility. *Environmental Challenges*, 22. <http://dx.doi.org/10.1016/j.envc.2026.101407>

N.B. When citing this work, cite the original published paper.



Removal of microplastics and metals in biochar beds for stormwater treatment: Effects of prolonged drying and salinity on pollutant mobility

Gabriella Rullander^{a,*}, Roger Herbert^a, Ann-Margret Strömvall^b, Jes Vollertsen^c, Claudia Lorenz^d, Sebastien Rauch^b, Amir Saeid Mohammadi^b, Sahar S. Dalahmeh^e

^a Department of Earth Sciences, Uppsala University, Villavägen 16, SE-752 36, Sweden

^b Water Environment Technology, Department of Architecture and Civil Engineering, Chalmers University of Technology, SE-412 96 Gothenburg, Sweden

^c Department of The Built Environment, Aalborg University, Thomas Manns Vej 23, 9220 Aalborg Øst, Denmark

^d Environmental Dynamics, Department of Science and Environment, Roskilde University, Universitetsvej 1, 11.2 DK-4000, Roskilde, Denmark

^e Department of Sustainable Development, Environmental Science and Engineering, KTH Royal Institute of Technology, Teknikringen 10b, SE-100 44, Stockholm, Sweden

ARTICLE INFO

Keywords:

Horizontal filters
Polar and non-polar polymers
Road dust
Sorption
Stormwater
Stormwater treatment

ABSTRACT

Biochar-based filters offer a promising solution for removing pollutants from stormwater, yet their performance under environmental stressors remains insufficiently studied. This study evaluated the efficiency of biochar beds in retaining microplastics (MPs) and metals under prolonged dry conditions and with increased salinity. Results showed that MPs were well retained through entrapment in biochar's porous structure, with non-polar polypropylene (PP) fragments removed more efficiently (98–99%) than polar polyamide (PA) fragments (83–92%). The MP retention improved over time, highlighting biochar's long-term filtration potential. However, a five-week dry period lowered effluent pH, consequently increasing metal mobility, while higher salinity events enhanced the dissolution of some metals, reducing their total removal. To simulate real-world conditions, semi-artificial stormwater was created by mixing road dust with deionized water. This mixture, along with virgin MPs, was introduced into biochar beds twice weekly under first-flush conditions. Effluent analysis of metals and MPs via inductively coupled plasma mass spectrometry (ICP-MS) and Fourier transform infrared spectroscopy (μ -FTIR imaging), respectively, confirmed the preferential retention of non-polar MPs and shifts in metal mobility. These findings emphasize the importance of considering environmental conditions and polymer characteristics when assessing biochar's filtration performance in practical applications.

1. Introduction

Urban areas, characterized by dense populations and impermeable surfaces such as rooftops and parking lots, can generate substantial stormwater runoff during rain events. Stormwater runoff is often described using a runoff coefficient (C), representing the fraction of rainfall that becomes surface runoff. For paved parking lots, values typically range from 0.7 to 0.9, with 0.8 often used (Göbel et al., 2007). This runoff is a major vector for transporting pollutants accumulated in road dust and debris (Müller et al., 2020). Among these pollutants, microplastics (MPs)—plastic particles smaller than 5 mm—have been recognized as a significant contributor to aquatic pollution through stormwater pathways (Shafi et al., 2024). Monira et al. (2021) estimated that up to 50 % of all MPs reaching recipient waters originate from road dust via stormwater transport. Urban sources of MPs include plastic

litter, wastewater overflows from combined sewer systems, and materials associated with construction and infrastructure. Additionally, leaching of additives from plastics (e.g., phthalates, plasticizers, UV stabilizers, and flame retardants) can pollute stormwater (Rosso et al., 2022). Urban traffic further exacerbates pollution through the release of organic pollutants like polycyclic aromatic hydrocarbons (PAHs), aliphatic hydrocarbons, and phthalates (Björklund et al., 2009; Markiewicz et al., 2017), as well as metals (Müller et al., 2020) and tire wear particles (TWPs; Gaggini et al., 2024).

Studies on MP concentrations in stormwater reveal significant variability, influenced by factors such as sample type, sampling methods, location, pretreatment and analysis techniques, and reported MP sizes. The last factor is critical, as MP concentrations tend to increase with decreasing particle size (Ivleva, 2021). For example, Swedish studies have reported MP concentrations of 51,000 MPs/L (>20 μ m) in

* Corresponding author.

E-mail address: gabriella.rullander@geo.uu.se (G. Rullander).

<https://doi.org/10.1016/j.envc.2026.101407>

Received 19 August 2025; Received in revised form 12 January 2026; Accepted 13 January 2026

Available online 14 January 2026

2667-0100/© 2026 The Author(s). Published by Elsevier B.V. This is an open access article under the CC BY license (<http://creativecommons.org/licenses/by/4.0/>).

washwater from a street-sweeping machine (Järnskog et al., 2021) and 5900 MPs/L (>20 μm) in urban stormwater (Järnskog et al., 2020). Another study found an average concentration of 24 ± 16 MPs/L (>50 μm) in roadside snowbanks (Vijayan et al., 2022), whilst a median concentration of 230 MPs/L (>20 μm) was observed in road runoff (Lange et al., 2022). These examples highlight the wide range of MP concentrations in the environment, emphasizing the importance of applying these concentrations in experimental MP studies. Stormwater quality is also influenced by factors like antecedent dry days and rain intensity, with first-flush events estimated to carry up to 80 % of the pollutant load within 30 % of the initial runoff volume (Saget et al., 1996). Despite these dynamics, experimental studies on MP stormwater treatment rarely incorporate these real-world complexities into their designs.

MPs have also been recognized as vectors for common stormwater metals (Liu et al., 2022) such as Cu, Zn, Pb, Co, and Cd, which originate from sources including rooftops, vehicle components, and Zn leakage from TWP in the urban environments (Müller et al., 2020). As vectors, MPs can increase the transport distances for metals in aquatic environments by remaining suspended longer than denser particles (Guan et al., 2020). However, the extent to which metals sorb to MPs is governed by surface interactions and the polarity of MPs in particular (Liu et al., 2021). This dual role of MPs, acting as both transport facilitators and potential sources of toxicity, raises concern regarding their environmental impact. While metal toxicity is well-documented (Eriksson et al., 2007), MPs pose risks through ingestion and toxic leaching (Campanale et al., 2020) associated with chronic diseases. Given their role in pollutant transport, a deeper understanding of how MP type and polarity affect retention in stormwater treatment systems is essential.

Stormwater pollutants pose risks to aquatic environments, leading many countries to adopt stormwater management strategies to improve water quality and quantity (Davis, 2005). Among these, filtration-based techniques, traditionally using sand as filter media, have demonstrated potential for MP removal (70–90 %; Lange et al., 2022; Lange et al., 2021; Smyth et al., 2021). At the same time, nature-based porous materials like biochar have emerged as promising alternative filter media, owing to their high porosity and surface area, which can enhance pollutant removal through physiochemical interactions (Tan et al., 2015). Biochar has been shown to effectively remove metals (Chen et al., 2022), hydrophobic contaminants like PAHs (Valizadeh et al., 2022), and MPs with a reported efficiency of 95–100 % (Johansson et al., 2024; Rullander et al., 2024; Wang et al., 2020). However, to the authors' knowledge, no studies have explicitly examined biochar's effectiveness in removing MPs across different polymer types.

As biochar gains popularity in filtration-based stormwater management, understanding its performance under environmental stressors, such as prolonged dry periods and Nordic winter conditions, becomes increasingly important. These external factors may not only influence biochar's ability to remove stormwater pollutants but also affect pollutant mobility. The sorption of dissolved metals, for instance, is particularly sensitive to external conditions like pH, organic content, and redox potential (Bradl, 2004), all of which can fluctuate with seasonal changes in stormwater discharge and quality. This was observed in bioretention filters amended with sorptive materials (Johansson et al., 2025), including biochar, which were exposed to extreme rain events under Nordic winter conditions. While these filters effectively removed MPs, their efficiency in removing Cu, Cr, and Zn was reduced (Johansson et al., 2025). Additionally, extended flow interruptions have been shown to cause peak releases of particles in porous media (Schelde et al., 2002), raising concerns about the long-term effectiveness of biochar-based treatment systems. Furthermore, road salt, commonly used in colder climates, has been demonstrated to promote the desorption of metals in traditional filter media (Paus et al., 2014). Electrostatic interactions between salt and MPs may further impact the mobility and aggregation of MPs, potentially altering their retention and role as vectors for metal transport (Antonson et al., 2021). These factors add

complexity to the performance of biochar filters and highlight the need for further research into their efficiency in mitigating MPs under varying environmental conditions.

Despite growing evidence that biochar can improve stormwater quality, important gaps remain concerning its performance under environmentally realistic stress conditions and for removal of emerging pollutants. In particular, no studies have evaluated biochar retention of MPs with contrasting polymer properties at a larger scale or in combination with commonly occurring stormwater metals. Natural stressors have likewise received limited attention. Multi-week dry periods, which commonly occur during Nordic summers, can influence particle release and metal mobility, while winter road-salt applications can elevate chloride concentrations from mg L^{-1} to g L^{-1} levels during first-flush snowmelt (Ekvall and Strand, 2001; Robinson and Hasenmueller, 2017). These conditions are therefore relevant for assessing biochar robustness. By integrating polymer-specific MPs with environmentally realistic drying and salinity stress, this study provides new insight into how biochar filtration performs under practical stormwater scenarios.

This study aims to assess the performance of pilot-scale biochar beds in removing MPs and metals from semi-artificial stormwater, particularly under environmental stress conditions. Specifically, the study investigates: i) The removal of road dust-derived MPs, polar and non-polar virgin MP fibers and fragments, and total and dissolved metals, and ii) The impact of environmental stressors (prolonged dry period and addition of road salt) on filter performance. By addressing these objectives, the study provides insights into the applicability of biochar beds for real-world stormwater management under varying environmental conditions.

2. Materials and method

The experimental study was conducted using two parallel pilot-scale filter boxes filled with biochar and operated under controlled laboratory conditions. The filters were supplied with artificial stormwater containing MPs and metals and were subjected to three operational phases: a normal operating period, a prolonged dry period without inflow, and a salt-impacted period simulating winter road-salt runoff. During simulated stormwater infiltration events, effluent samples were collected to assess MP and metal breakthrough from the filters.

2.1. Biochar, road dust, and microplastics

Commercially obtained biochar, primarily derived from pine with contributions from birch, alder, and aspen hardwood, was used as the sorbent material. It was produced under low-oxygen conditions at 500 °C for 8–14 h (Vindelkol AB, Sweden). A sieved mixture of 1–5 mm particle sizes was selected, composed of 50 % (w/w) particles at 1–1.5 mm, 30 % (w/w) at 1.5–2.5 mm, and 20 % (w/w) at 2.5–5 mm. The biochar's porosity (87 ± 0.010 %) and specific surface area (158 ± 1.77 m^2/g) were determined using the Brunauer-Emmett-Teller (BET) method. Road dust grab samples were collected along curbs at two commercial parking lots in Uppsala (coordinates: 59.877352, 17.676267; 59.847863, 17.693326; WGS84 decimal) using a metal ladle and stored in glass jars. To match previous studies, road dust was sieved to exclude particles >500 μm . Organic content was determined by loss on ignition (550 °C for 5 h). The bulk and sieved road dust, categorized by size (<20, 20–40, 40–60, 60–125, 125–250, 250–500, >500 μm), were analyzed for metal content via inductively coupled plasma mass spectrometry (ICP-MS). The particle size distribution of the sieved road dust and biochar mixture was analyzed (see Supplementary Information Figure S1), and their composition was determined using X-ray fluorescence (XRF, Tracer 5i, Bruker) and Energy Dispersive X-ray Analysis (EDAX) (see Supplementary Information S2).

In addition to metals, road dust contained MPs, which were extracted and identified using Fourier transform infrared spectroscopy ($\mu\text{-FTIR}$ imaging), confirming the presence of various types of MPs. Alongside

the naturally occurring MPs in the road dust, virgin MPs were used in the experiment, including fibers and fragments of non-polar polypropylene (PP) and polar polyamide (PA 6.6). PP and PA were selected to represent contrasting polymer polarities, with PP also being the dominant polymer identified in the analyzed road dust ($\approx 83\%$). These polymers were also commercially available in comparable particle sizes (fragments and fibers), which was important for experimental consistency. The choice to include only these two polymers constitutes a simplification relative to the full diversity of MPs typically found in stormwater. Furthermore, the virgin PP and PA particles used here do not account for weathering, including surface oxidation, found in environmental MPs, which may influence sorption and retention. These factors should therefore be considered when interpreting the representativeness of the results.

The PP and PA fragments (MP Solutions, France) had average sizes of $35\ \mu\text{m}$ and $34\ \mu\text{m}$, respectively. The fibers had the following dimensions: PP fibers (Goodfellow, England) were $38\ \mu\text{m}$ in width and $331\ \mu\text{m}$ in length, while PA fibers (MP Solutions, France) were $41\ \mu\text{m}$ in width and $270\ \mu\text{m}$ in length (Supplementary Information Table S2). Using μFTIR imaging, the virgin MP concentration in ethanol suspension was quantified, allowing for a more controlled addition of virgin MPs to the biochar beds during each event.

2.2. Biochar bed set-up

Two pilot-scale horizontal boxes (F1 and F2) with a size $100 \times 20 \times 45\ \text{cm}$ were constructed and filled with biochar media (Fig. 1). The boxes were made of 10 mm Plexiglas and packed with biochar, with 10 cm crushed rock (granite, 8–16 mm) on top of the biochar to prevent buoyancy and provide water distribution, erosion protection, and pre-filter larger suspended solids at the inlet. Additionally, Plexiglas walls ($20 \times 25\ \text{cm}$) directed the water deeper into the biochar bed. The primary sampling point for effluent was located 5 cm from the top of the bed, with four additional sampling points across the bed's horizontal length, using Plexiglas tubes (20 cm long, 5 cm diameter) with 0.5 cm spaced holes (Fig. 1). These tubes were filled and layered with rock material to maintain a continuous water flow and prevent drainage of

biochar particles. During operation, the biochar beds were kept fully saturated with water, except when investigating the impact of drying or during brief intervals between test periods (*Normal*, *Dry*, and *Salt*) when the biochar bed was emptied via the additional sampling points. Water samples were collected from these points via taps installed on the side.

2.3. Design of stormwater events and synthesis of semi-artificial stormwater

Each stormwater event simulated runoff from a $2.66\ \text{m}^2$ catchment area, based on a 3% bioretention cross-sectional area to catchment area ratio (Hunt et al., 2012). The event modeled 20 mm of rain over 160 min, representing a 2-year return period (see Supplementary Information S3), with an estimated runoff coefficient of 0.8 for paved parking lots. Consequently, each event involved 43 L of semi-artificial stormwater entering the biochar beds at a flow rate of 0.27 L/min over the 160-minute duration.

Semi-artificial stormwater was prepared based on Milovanovic et al. (2023) with modifications, and it was applied to the biochar beds in two stages to simulate pollutant distribution in first flush events. Each event used 48 g of road dust and 43 L of deionized (DI) water, achieving an average total suspended solids (TS) concentration of 1.1 g/L. To mimic the first flush, 80% of the total road dust mass (38 g) was mixed into 13 L of DI water and applied first, followed by the remaining 20% (10 g) in the next 30 L. The stormwater was stored in a covered 100 L glass box and pumped into the biochar beds via a peristaltic pump (Masterflex L/S Labinette, Sweden), while being manually mixed with a glass rod every $\sim 5\ \text{min}$. At the start of each stormwater event, in addition to naturally occurring MPs from road dust, a controlled mixture of virgin MPs (PP and PA fibers and fragments) was introduced at the biochar bed inlets to assess the effects of shape and polarity on MP retention. For consistency with the first flush approach, 80% of the total MP count was introduced before the initial 13 L addition, with the remaining 20% added before the subsequent 30 L stormwater phase.

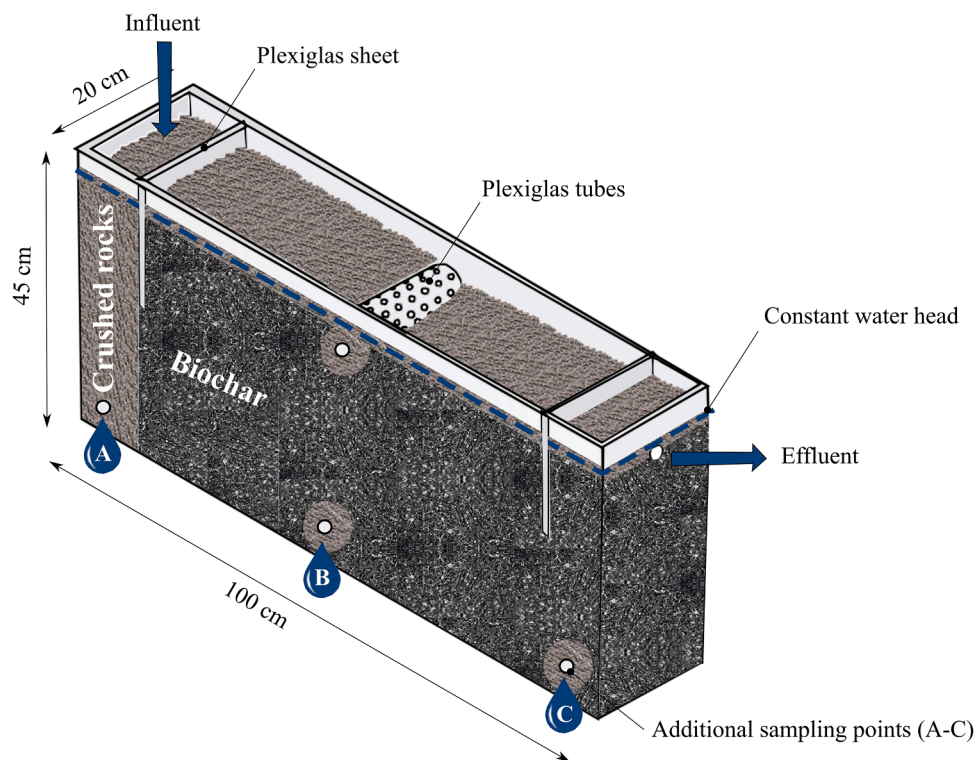


Fig. 1. Schematic illustration of the pilot-scale laboratory biochar bed set-up.

2.4. Experimental run

The experiment was conducted in duplicate pilot-scale biochar beds (Figure 1; F1 and F2), and all three experimental periods (*Normal*, *Dry*, and *Salt*) were carried out in duplicate using these two parallel beds. The experiment ran across three consecutive periods: a normal period (Period 1, *Normal*), a prolonged drying period (Period 2, *Dry*), and a road salt application period (Period 3, *Salt*). For period 2, a five-week drying period was applied to represent extended no-flow conditions that can occur during Nordic summers, as multi-week precipitation deficits have been observed in central Sweden and are projected to become more frequent under future climate change (Sjökvist et al., 2015). For period 3, a three-week period of saline water application simulated an episode of highly saline runoff during snowmelt. During such episodes, chloride concentrations have been reported ranging from mg L^{-1} to g L^{-1} with values exceeding $1\,000\text{ mg L}^{-1}$ near salted roads (Shetty et al., 2020); extreme concentrations up to $11\,800\text{ mg L}^{-1}$ have been measured in roadside snow slush (Novotny et al., 1998). Based on these observations, a NaCl concentration of 4 g L^{-1} was selected to represent an extreme but environmentally relevant salinity event. While natural precipitation patterns do not follow the exact alternating sequence imposed experimentally, the applied conditions capture plausible hydrological extremes relevant to stormwater systems under climate variability and change.

In the *Normal* period, semi-artificial stormwater events, as described above, were added twice a week, for a duration of three weeks (Fig. 2). At times when water was not added to the biochar beds, no flow occurred. After this, the biochar beds were emptied of water through the extra sampling points and left to dry for 5 weeks at the start of the *Dry* period. Following this drying phase, one stormwater event using only DI water was introduced, with water samples collected in six-volume increments to assess any potential pollutant release induced by the drying process. After this single DI water event, artificial stormwater was reintroduced for two weeks (Fig. 2). In the *Salt* period, sodium chloride (NaCl, 4 g/L) was incorporated into the semi-artificial stormwater for two stormwater events during the first week. The biochar beds then continued to receive regular semi-artificial stormwater for an additional two weeks (Fig. 2). In total, 731 l of artificial stormwater and DI water (43 L) were added to the biochar beds during the experiment, corresponding to approximately 17 pore volumes.

2.5. Sampling of influents and effluents over the experimental periods

For each event, influent and effluent samples were collected during

the experimental periods (Fig. 2) to analyze dissolved COD, turbidity, pH, dissolved and total metal concentrations, and MP abundance and composition (Fig. 3). An overview of the experimental replication, number of stormwater events, and effluent sampling scheme for each operational period is provided in Supplementary Table S3.

2.5.1. Influent

At the start of each event, three 1 L grab samples were collected using glass beakers from a single, well-mixed stormwater source to ensure identical influent conditions for both biochar beds and to measure dissolved and total metals and turbidity (Fig. 3, point a). Turbidity was measured on all three grab samples due to the simplicity of the analysis. The grab samples were subsequently combined for pH determination, and a subsample was filtered ($0.45\text{ }\mu\text{m}$ PES) for COD analysis (Fig. 3, point b). Combined samples were used for influent pH and COD since these properties were expected to be homogeneous within the source water and in order to conserve analytical resources over the extended experimental period. The collected grab samples were therefore used to support different analyses and were not intended as analytical replicates. Any remaining water was returned to the stormwater source. To evaluate MP content in the influent, a total of 100 g of subsampled road dust was analyzed and extracted for MPs (see Section 2.7.2).

2.5.2. Effluent

Two effluent sample types were collected per event: a total effluent sample and two 1 L grab samples. The total effluent sample was collected in metal buckets via silicone tubes for subsequent filtration and MP analysis (Fig. 3, point g). Grab samples were collected over the first half (0–80 min) and the second half (80–160 min) of each event (Fig. 3, points d and e). These were analyzed for dissolved and total metals and turbidity, then combined for pH measurement and COD analysis (Fig. 3, point f). For the *Normal* period, MPs in the total effluent were measured in two volume increments: during the first flush (13 L) and during the remaining effluent (30 L). During the *Normal* period, effluent was fractionated to assess potential differences between first-flush and later effluent. As no consistent differences in MP retention were observed, effluent from subsequent *Dry* and *Salt* periods was collected as a single composite sample (43 L, Fig. 3, point g) per event to obtain an event-integrated representation of pollutant release while reducing analytical complexity. After each period (*Normal*, *Dry*, and *Salt*), the biochar beds were drained via the additional ports, where 1 L grab samples were taken for dissolved and total metal analysis (Fig. 3, point c). See Supplementary Table S3, for a summary overview.

Unless otherwise stated, all analytical results represent single

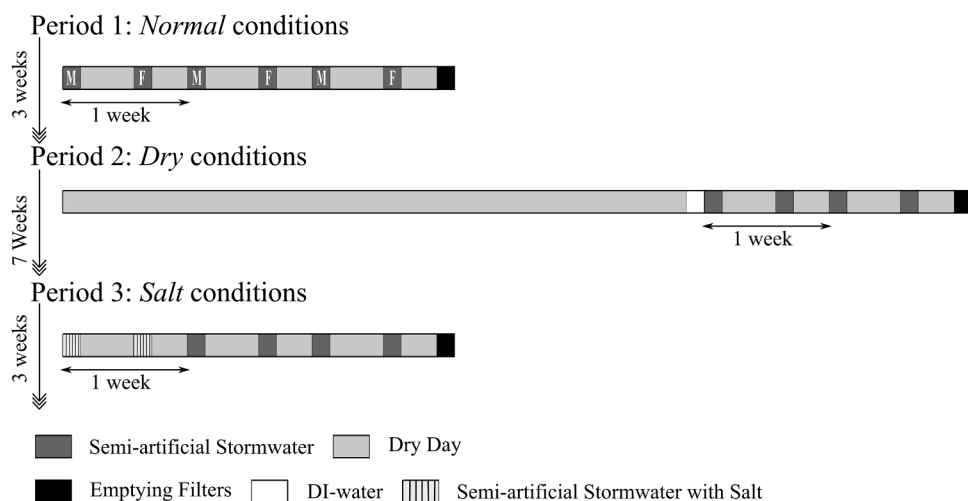


Fig. 2. Timeline of the experimental run, showing stormwater events and sampling on Monday (M) and Friday (F) for each operational period, along with specific conditions for each period.

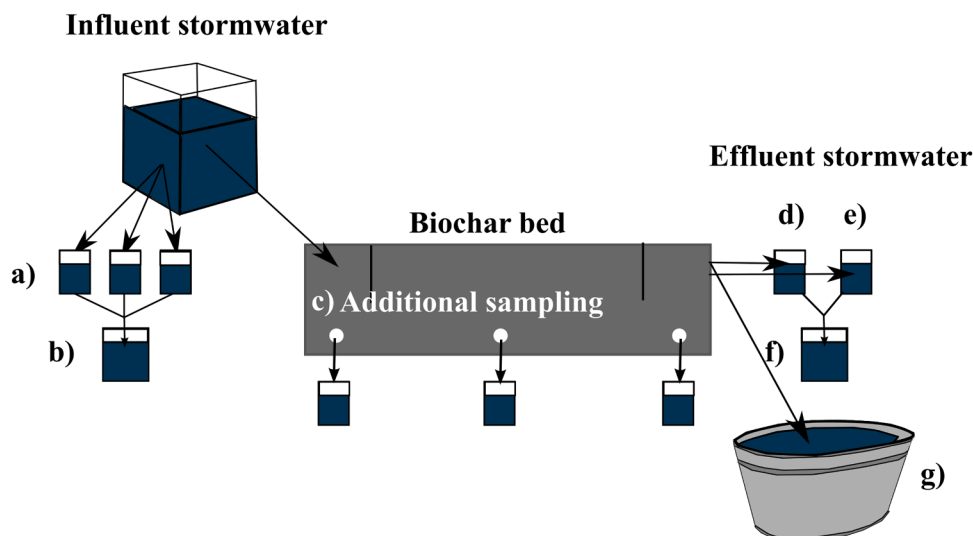


Fig. 3. Simplified schematic of sampling for each stormwater event for Periods 1–3 (*Normal, Dry, Salt*). Influent stormwater sampling is conducted at points (a) and (b), effluent sampling at points (d) – (g), and additional sampling at points (c).

measurements per event and per biochar bed and are therefore treated as independent measurements rather than analytical replicates. However, the experimental setup comprised two identical biochar beds operated in parallel under identical conditions and is therefore considered a duplicate experiment. Due to the time-intensive nature of μ -FTIR imaging and the large effluent volumes required, MP analyses were performed once per event and per biochar bed using composite effluent samples; MP results thus represent event-based observations and are presented separately for each biochar bed, which behaved independently. For metals, both dissolved and total concentrations were determined from two grab samples per event and per biochar bed. Subsequent statistical analysis showed no significant differences between the two biochar beds (see Results), and metal data were therefore combined for further analysis.

2.6. Hydraulic residence time determination

The hydraulic residence time was measured before the *Normal* and after the *Salt* periods using a sodium chloride (NaCl, 4 g/L) solution, representing approximately 5 % (2 L) of the pore volume. The solution was injected at 0.27 L/min for approximately 8 min. Effluent conductivity was monitored every 1–5 min with a conductivity probe (Tetracond 325, WTW) connected to a conductivity meter (Cond 3310, WTW). The mean residence time, corresponding to the detention period within the biochar beds, was defined as the time for the breakthrough of 50 % of the injected salt mass (see Supplementary Information Figure S2).

2.7. Analysis

2.7.1. pH, turbidity, COD, and metals

Throughout the experiment, pH, turbidity, and COD were measured using a pH meter (VWR pH 1100 L), a turbidimeter (Hach 2100Q), and a COD test kit (Merck 1.14540.0001) with a spectrophotometer (Merck Spectroquant Nova 60 A). For total metal analysis, water samples (10 mL) were stored in 15 mL metal-free centrifuge tubes (VWR), acidified with 1 % nitric acid (70 % HNO₃, ≥ 99.999 % trace metal grade, Sigma-Aldrich), and digested before analysis. The dissolved metals were determined by filtering water via sterile 0.45 μ m PES syringe filters (VWR), after which 10 mL of the filtrate was also acidified. Metal analysis was performed using ICP-MS (Thermo Fischer Scientific ICAP Q) with a FAST sample introduction system (Elemental Scientific) and He as collision gas. Nine metals (Fe, Mn, Pb, Cd, Cr, Co, Cu, Zn, and Ni) were analyzed throughout the experiment.

2.7.2. Microplastic extraction and identification

MP extraction from road dust followed a modified method from Iordachescu et al. (2024). Road dust was sieved (<500 μ m), and potential MPs (>500 μ m) were manually picked for visual inspection. These MPs were suspected to originate from carrying bags, cigarette butts, fiber threads, tire wear particles, and other sources (see Supplementary Information Figure S3). For the smaller fraction, 10–20 g of the fine particles was transferred to separatory funnels, and mixed with ZnCl₂ (1.7 g/cm³) using compressed air. The mixture was allowed to settle overnight, after which the settled materials could be discarded via the bottom valve. This process was repeated over several days. To minimize MP loss, the discarded materials underwent a second density separation, and the recovered supernatants were reintroduced into the original matrix. The final supernatant was filtered through 10 μ m stainless steel filters, and the retained materials were subjected to a Fenton reaction in an ice bath using 345 mL of 33 % H₂O₂, 65 mL of 0.1 M NaOH, and 0.1 M FeSO₄. After 24 h, samples were again filtered at 10 μ m and underwent a final density separation, as described above. The resulting supernatant was filtered at 10 μ m, and the MPs were dislodged from the filters via ultrasonic treatment in ethanol. The final MP-ethanol suspension was then transferred to 20 mL glass vials, and the ethanol was evaporated. MP extraction from biochar bed effluents was more straightforward. The collected effluent water was filtered through 10 μ m stainless steel filters using a vacuum pump. The filters were submerged in ethanol, and the particles were dislodged via sonication before being stored in 20 mL glass vials, as previously described. Before μ FTIR imaging, all sample volumes were standardized by adding 2–5 mL of ethanol.

To ensure contamination control, all materials (e.g., filter disks, beakers, and Petri dishes) were made of metal or glass and sterilized before use. Vinyl gloves, cotton lab coats, and fume hoods were employed during MP extraction. The inlets and outlets of the filters, as well as stainless-steel buckets collecting effluents, were covered with aluminum foil to prevent airborne MP deposition. To monitor atmospheric contamination, a glass beaker filled with 100 mL of tap water was placed next to the filters and later analyzed for MP content, and a background control of a total of 86 L was sampled for MPs. In the sub-samples for inadvertent contamination, 10 MPs were identified (PET>PA>PE>PP), and a correction was deemed inappropriate (see Supplementary Information Figure S4 for details). Additionally, to avoid interference from the filter setup, PMMA was excluded from the MP analysis.

Extracted particles were quantified and identified using μ -FTIR

imaging. The MP-ethanol suspensions were homogenized (60 s, vortex stirrer) and deposited onto 13×2 mm zinc selenide (ZnSe) transmission windows (Crystran, UK) within a 10 mm active area, mounted in a micro-compression cell (Pike Technologies, USA). Samples were dried at 40°C before analysis. Chemical characterization was conducted using a Cary 620 FTIR microscope coupled with a Cary 660 IR spectrometer (Agilent Technologies, USA), equipped with a $15 \times$ Cassegrain objective and an FPA detector (64×64 , $5.5 \mu\text{m}$ pixel resolution). Samples were scanned in transmission mode ($3750\text{--}850 \text{ cm}^{-1}$, 8 cm^{-1} resolution) with 30 co-added scans per pixel. A 120-scan background was collected before each analysis to ensure spectral precision.

2.8. Data handling

FTIR spectral maps were analyzed using siMPle v.1.3.1 β (Primpke et al., 2020) for semi-automated matching against a reference library, including study-specific virgin MPs. Identified MPs were classified by polymer type, size, and shape. Particle length, width, and estimated mass were determined using elliptical geometry, polymer densities, and a thickness assumption of 60 % of the minor dimension. Fibers were defined as particles with an elongation factor >3 (Vianello et al., 2019). TWPs were excluded from analysis, as their high carbon black content prevents detection by μFTIR analysis. All statistical analyses were performed in MATLAB (R2021a). The normality of metal concentrations and MP counts was assessed with the Shapiro-Wilk test. Due to non-normal distributions, the Mann-Whitney U test compared metal concentrations and physiochemical parameters between replicate biochar beds. Event-based metal concentrations (total, dissolved, particulate) were compared using the Wilcoxon signed-rank test to assess treatment-related changes. MP length and width were analyzed using the Kruskal-Wallis test, followed by Dunn's post-hoc test. Spearman correlation was used to examine relationships between effluent metal and MP data. Statistical significance was assessed at the level of $\alpha=0.05$.

3. Results and discussion

3.1. Elemental composition and metal distribution in road dust

The analysis of bulk road dust samples revealed that metal concentrations increased in the order of $\text{Co} < \text{Pb} < \text{Ni} < \text{Cu} < \text{Cr} < \text{Zn} < \text{Mn} < \text{Fe}$, ranging from 11 ± 3.9 to $27,000 \pm 5400 \mu\text{g/g}$, with Cd below the limit of quantification ($0.18 \pm 0.04 \mu\text{g/g}$) and a clear trend for increasing metal

concentrations with decreasing particle size (see Supplementary Information Table S4). The elemental composition of the road dust indicated a mineral-based material with potential contributions from anthropogenic sources such as road salts or urban infrastructure (See Supplementary Information S2). The road dust had a low organic material content ($2.5 \pm 0.05 \%$ TS) as revealed by loss on ignition.

3.2. pH, COD, and turbidity

The biochar beds exhibited similar trends in turbidity, pH, and COD over the three sampling periods, with no statistically significant differences observed between the replicate systems ($p > 0.05$). Effluent turbidity was consistently lower than the influent, and declined over the *Normal*, *Dry*, and *Salt* periods, indicating that the biochar bed filtration efficiency improved over time (Fig. 4). However, at the start of the *Dry* period, an initial turbidity spike was observed, likely due to particle release after extended drying, but it quickly subsided with subsequent flushing. By the *Salt* period, turbidity remained low and stable, demonstrating sustained filter performance even with road salt exposure. It is important to mention that turbidity measurements do not indicate the specific type of particles detected, meaning that elevated effluent readings could reflect not only stormwater particles but also potential biochar release. However, effluent turbidity in the control samples, collected before the start of the experiment, was lower than in the *Normal* period, suggesting that the measured turbidity primarily originated from stormwater. Compaction of stormwater filters during startup has also been observed in previous studies (Johansson et al., 2024; Ghavanloughajar et al., 2020), and such compaction may also explain the faster breakthrough times observed in the tracer test at the end of the experiment (Supplementary Information Figure S2).

The COD concentrations in the biochar bed effluents consistently exceed those in the influent (Fig. 4), showing an increasing trend during the *Normal* period, followed by a gradual decline over the *Dry* and *Salt* periods. This pattern is consistent with previous findings that biochar-amended filters can leach organic carbon (measured as dissolved organic carbon, DOC), with the extent of leaching influenced by the amount of biochar used (Mukherjee and Zimmerman, 2013). As filters continue to operate, this leaching tends to decrease (Youngwilai et al., 2022). Given the high biochar content in the biochar beds, the elevated COD concentrations in the effluents are likely attributable to organic carbon leaching (Fig. 4).

During the *Normal* period, the pH of both influent and effluent

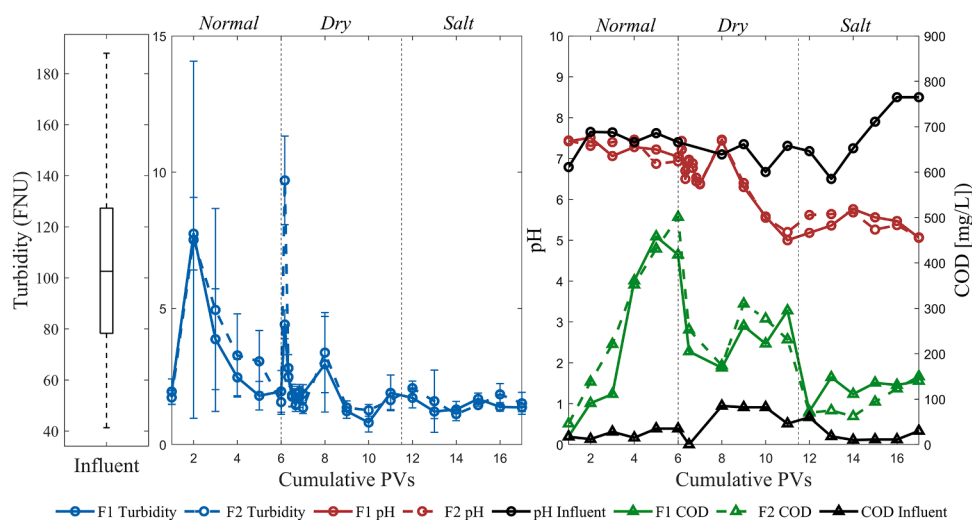
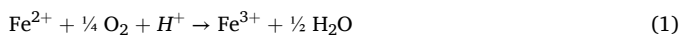


Fig. 4. Water quality parameters during Periods 1–3 (*Normal*, *Dry*, and *Salt*). Left panel, turbidity for influent stormwater (boxplot). Middle panel, effluent turbidity from biochar beds F1 and F2. Right panel, influent and effluent pH (left y-axis), and COD (right y-axis), for F1 and F2. One pore volume corresponds to one stormwater event. For each biochar bed, turbidity was measured three times per event, whereas COD and pH effluents are unique values per event.

stormwater remained near neutral (Fig. 4). However, following the prolonged drying period, effluent pH declined, dropping to around 5 by the end of the *Dry* period. The pH drop following prolonged drying is suggested to be linked to the high Fe content in the road dust (see Supplementary Information Table S4). Ferrous iron (Fe^{2+}) is sensitive to oxidation (Jolivet et al., 2004), and increased oxygen levels during drying likely promoted its conversion to ferric iron (Fe^{3+} ; reaction 1). This, in turn, led to the formation of ferric hydroxide ($\text{Fe}(\text{OH})_3$) precipitates (Calugaru et al., 2018) (reaction 2), which were visible as ochreous deposits near the inlets and as colored water at the outlets. The ferric hydroxide colloids were later flushed out during the *Salt* period. The overall oxidation and precipitation reactions are acid-generating, likely contributing to the observed decline in pH (Fig. 4).



3.3. Microplastics in semi-artificial stormwater

Road dust extractions revealed that up to 2700 MP counts were introduced to the biochar beds per semi-artificial stormwater event, resulting in an approximate stormwater concentration of 60 MP counts/L, with PP comprising the majority (83 %) of the polymer distribution, followed by PE (13 %) and a mix of PA, PVC, PS, and PET (6 %; Fig. 5). These results align with those of Iordachescu et al. (2024), who reported 4 to 300 MP counts per gram of road dust from commercial parking lots in Uppsala, with PP as the dominant polymer (32–79 %) followed by PE. Similar to this study, they also detected PA, PVC, PS, and PET. Each stormwater event also included a controlled addition of virgin MPs, as described in the Method section. This contributed an estimated 1000–1300 PA and PP fibers and 3500–4200 PP and PA fragments per event, resulting in an extra MP load of 258 counts/L (80 fibers/L, 178 fragments/L). When combined with MPs derived from road dust, the total MP load in the semi-artificial stormwater reached 320 counts/L,

resulting in an approximate dose of 14,000 MPs per event. It is important to note that due to identical polymer compositions, μFTIR imaging could not distinguish between road dust-derived and virgin PP and PA fragments. However, siMPLe-based size analysis revealed consistent differences between the two sources. For example, road dust-derived PP fragments were generally larger (124 μm in length, 74 μm in width) than the virgin fragments, indicating differing sources despite the chemical similarity.

3.4. Microplastic retention over all periods

Retention patterns for both road dust-derived and virgin MPs across

Table 1

Microplastic removal efficiencies* (%) across the whole experiment with all periods included, and for individual periods (*Normal*, *Dry*, and *Salt*), for biochar beds F1 and F2 (N.A.=not available). Removal efficiencies are calculated from event-based composite $\mu\text{-FTIR}$ measurements performed once per event and per replicate biochar bed; values represent observed event-based removal and are not mean values.

	Normal		Dry		Salt		Average of all periods	
	F1	F2	F1	F2	F1	F2	F1	F2
PA Fiber [†]	99	100	100	100	100	100	100	100
PA Fragments [†]	83	70	96	81	97	99	92	83
PE	95	87	100	98	96	100	97	95
PET	98	99	100	100	100	100	100	100
PP Fiber [†]	100	100	99	100	100	100	100	100
PP Fragments [†]	98	98	98	98	99	100	99	98
PS	100	80	100	100	100	100	100	93
PU	N.A	N.A	N.A	N.A	N.A	N.A	N.A	N.A
PVC	87	91	100	-13	-64	100	34	68

[†] Only accounts for the removal of intentionally added virgin MPs.

$$* \text{Removal}(\%) = \frac{MP_{SIN} - MP_{SOUT}}{MP_{SIN}} * 100.$$

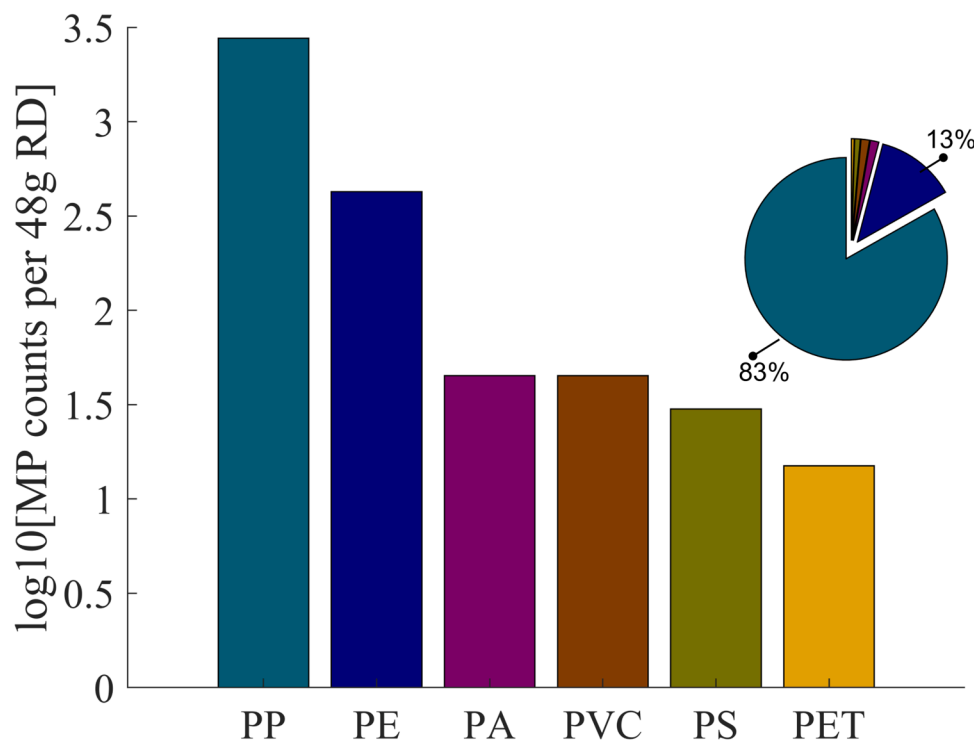


Fig. 5. The expected type and count of MPs in a stormwater event related to the addition of 48 g of road dust. The counts of MP types are displayed on a log scale. The pie chart shows the detailed distribution of the MPs.

all experimental periods are summarized in Table 1. The PP and PA measured in the effluents had an average size of 45 μm in length and 28 μm in width, closely matching the dimensions of the virgin MPs. In contrast, road dust-derived PP and PA were generally larger. Therefore, when calculating retention values of PP and PA (Table 1), only the known influent concentrations of the virgin PP and PA fragments were considered, as the effluent particles were more representative of this source. This approach was intentionally conservative, as to avoid overestimation of removal efficiencies. Of the total MP counts extracted from the biochar bed effluents, only 6 % consisted of MPs other than PP and PA. These included PE, PET, PS, PVC, and PU, originating from the semi-artificial stormwater source. Notably, PU was identified in the effluent, despite being absent in both the influent semi-artificial stormwater (Fig. 5) and the biochar beds effluent controls using DI water. However, PU has previously been detected in road dust from parking lots in Uppsala (Iordachescu et al., 2024). This suggests that PU was likely present in the heterogeneous road dust mixture but not captured in the specific influent subsamples analyzed, and is therefore not attributed to release from the biochar material.

During the *Normal* period, both biochar beds showed high removal efficiencies. Among the road dust-derived MPs, PE, PET, PS, and PVC were removed at 80–100 % (Table 1). For the virgin MPs, PP fragments were consistently retained at 98 %, while PA fragments showed lower removal efficiencies, ranging between 70 % and 83 %. In contrast, fiber retention was consistently high for both polymers, with both PP and PA fibers exhibiting 99–100 % retention.

During the *Dry* period, incremental sampling following prolonged drying revealed an initial release of MPs, particularly from one biochar bed, which was also reflected in the turbidity measurements (Fig. 4). Despite this initial release, retention performance recovered rapidly in subsequent stormwater events. The removal of PE in the *Dry* period increased to 98–100 %, while PET and PS were fully retained in both biochar beds (Table 1). The retention of PVC, however, was highly variable, showing complete removal in one replicate and a net release in the other. This variability, including the noted negative removal, may be explained by the low and heterogeneous influent PVC loads, where even a small desorption or remobilization of previously retained particles, particularly after the *Dry* period, can produce a net release. The retention of virgin PP fragments on the other hand, remained stable at 98 % across both biochar beds, while the virgin PA fragment retention improved, ranging from 81 % to 96 %. Fiber removal remained consistently high for both PA and PP, showing similar retention as in the *Normal* period (Table 1).

During the final *Salt* period, most MP types continued to be effectively removed, with slight improvement of the performance. Retention of PE reached 96 % and 100 %, and similar to the *Dry* period, PET and PS were completely retained. The retention of PVC once again showed variation: one replicate retained 100 %, while the other exhibited a net release. At this stage, virgin PP fragment retention increased slightly, while PA fragments reached their highest retention of the study at 97–99 % (Table 1). Similar to the *Normal* and *Dry* periods, PP and PA fibers were completely retained in the biochar beds.

Differences in MP retention across polymer types and morphologies suggest that both MP properties and MP dimensions influence removal efficiency. Virgin PP fragments were more effectively retained than virgin PA during the *Normal* period, indicating a potential retention preference for certain polymer types, specifically PP, by the biochar media. In contrast, the relative removal of PA varied across experimental periods, suggesting that changes in water chemistry, such as reduced pH and the addition of road salt, may have influenced the interaction between PA and the biochar surface. Additionally, the consistently high removal of fibers, with minimal breakthrough observed, highlights the role of particle shape and size in retention, likely due to the elongated structure of fibers enhancing physical filtration. These findings point toward both size-dependent and polymer-type-dependent mechanisms of removal, which are therefore

further examined in the following section.

3.5. Potential factors influencing microplastic retention

The experimental data show that MP particles detected in the effluent generally decreased in size over time and that retention efficiencies differed between polymer types, with consistently higher retention of PP than PA fragments. In the following section, these observed patterns are discussed in relation to potential physical and chemical retention mechanisms, drawing on previous literature, as the underlying mechanisms were not directly measured in this study.

The size and morphology of MPs appear to influence their removal efficiency in biochar beds. A significant difference in length and width was observed between MPs in the influent and those in the effluents from the *Normal*, *Dry*, and *Salt* periods ($p < 0.05$). Effluent MP sizes also varied between periods, with significant differences between *Normal* and *Salt*, and between *Dry* and *Salt*. This suggests that MPs in the influent and effluent were generally similar in size, but that filtration removed larger particles over time (Fig. 6). This trend likely reflects enhanced size-based retention resulting from progressive filter clogging, as reported in previous studies (Wang et al., 2020). Additionally, biochar has been shown to improve MP removal compared to traditional sand media (Tong et al., 2020), in part because progressive clogging of pore spaces increases the likelihood of physically trapping larger particles (Ahmad et al., 2023), but also because biochar's fragile structure may fragment over time, potentially promoting entanglement of MPs (Wang et al., 2020).

The results also indicate that in addition to size and morphology, polymer type and associated chemical characteristics could have affected MP retention. For instance, while both PP and PA fibers were consistently removed at >99 % efficiency, their fragment counterparts showed differing behavior. As shown in Fig. 7, both biochar beds exhibit a decreasing trend in MPs per liter of effluent over time. However, PP fragments, being non-polar and hydrophobic, were retained with high efficiency (98–100 %) throughout the experiment (Table 1). In contrast, the equivalent-sized PA fragments, which are more polar and contain functional groups capable of hydrogen bonding, showed lower and more variable retention, particularly during the *Normal* period (Fig. 7).

The biochar used in this study was produced at ~ 500 °C and is therefore expected to possess a relatively low oxygen-to-carbon (O/C) ratio and a hydrophobic surface. These characteristics were not identified directly in the current study but are well-documented for similar types of biochar (Yaashikaa et al., 2020), which provides a plausible explanation for the favored retention of non-polar MPs like PP. In contrast, the retention of more polar MPs like PA may depend on the availability of surface functional groups (e.g., hydroxyl or carboxyl groups) capable of hydrogen bonding (Mota et al., 2025). However, since this study did not include surface functional group characterization of either the biochar or the MPs, this interpretation is offered as a literature-based mechanism to contextualize the observed retention patterns.

The observed variations in PA retention across the different periods (Fig. 7), further suggest that environmental stressors such as drying and road salt exposure may have influenced removal. For example, during the *Normal* period, both the biochar and MPs are expected to carry negative surface charges at near-neutral pH, based on reported point of zero charge (PZC) values, potentially generating an electrostatic repulsion between the materials. While the PZC of similar pine-derived biochars has been reported between pH 5.6 and 5.8 (Bashir et al., 2022; Paul et al., 2020), and PP and PA typically have PZCs around pH 4.0 (Vieira et al., 2021), this study did not measure zeta potentials, and should therefore be interpreted as a plausible mechanism rather than a validated process. It is also possible that the slight acidification following the *Dry* period may have decreased the effect of charge repulsion, potentially contributing to the improved retention of PA fragments relative to the *Normal* period.

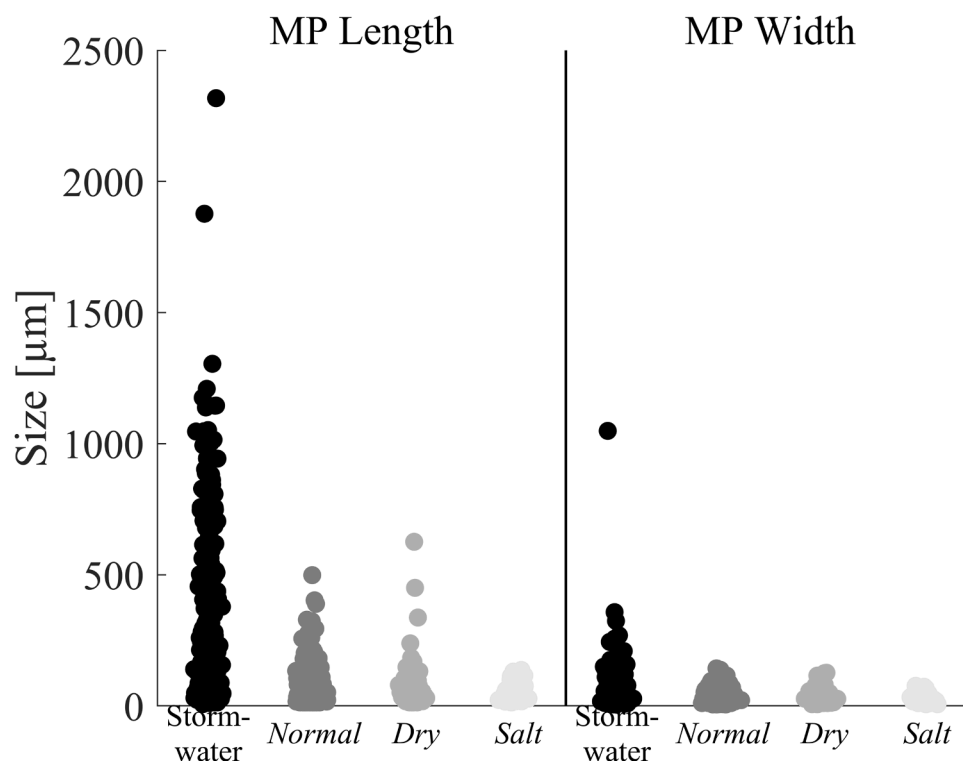


Fig. 6. Length and width distributions for MPs, determined by μ -FTIR, extracted from sieved road dust ($< 500 \mu\text{m}$) and virgin MPs in the stormwater, and effluent data collected during the *Normal*, *Dry*, and *Salt* periods. Effluent distributions represent pooled particle data from both replicate biochar beds (F1 and F2) for each period, which showed no appreciable variability in MP characteristics and were therefore combined.

The addition of road salt during the *Salt* period introduced further complexity. The increase in ionic strength, along with fluctuating pH, may have altered sorption dynamics in the biochar beds. While our findings indicate enhanced retention of PA under salt conditions, they contrast with those of Mota et al. (2025), who suggested that Na^+ and H^+ competition may reduce MP sorption. Overall, the differences observed in the retention of PP and PA across the three periods are therefore consistent with sorption dynamics, which is governed by hydrophobic interactions as well as electrostatic effects that vary with pH and ionic strength. However, these mechanisms were not measured directly and serve only to contextualize the empirical retention data. Future studies should include zeta potential analyses of biochar and MPs under stormwater-relevant conditions to directly test these mechanistic interpretations.

3.6. Influent metal concentrations and speciation

Table 2 presents the median total metal concentrations in influent stormwater during the *Normal*, *Dry*, and *Salt* periods, showing values consistent with typical urban stormwater (Göbel et al., 2007; Zgheib et al., 2012). These concentrations also align with recent data from Gothenburg, Sweden, where Johansson et al. (2024) reported urban stormwater metal ranges: Cd ($< 0.10 \mu\text{g/L}$), Co ($1.1\text{--}18 \mu\text{g/L}$), Cr ($5\text{--}30 \mu\text{g/L}$), Cu ($27\text{--}59 \mu\text{g/L}$), Fe ($760\text{--}8200 \mu\text{g/L}$), Mn ($76\text{--}670 \mu\text{g/L}$), Ni ($2.2\text{--}10 \mu\text{g/L}$), Pb ($1.2\text{--}4.9 \mu\text{g/L}$), and Zn ($80\text{--}250 \mu\text{g/L}$). For most of the experiment, a high proportion of metals in influent were particulate-bound (Table 2), likely due to the inclusion of road dust in the semi-artificial stormwater, which provides abundant surfaces for metal sorption, with similar proportions observed in natural stormwater (Johansson et al., 2025; Flanagan et al., 2018; Lange et al., 2022). However, during two events at the start of the *Salt* period, the addition of road salt (NaCl , 4 g/L) to the semi-artificial stormwater reduced the particulate fraction of metals, most notably for Co (67 %; Table 2). This outcome is consistent with the known effect of salt ions displacing

particle-bound metals, shifting them toward the dissolved phase (Marsalek, 2003).

3.7. Metal removal efficiencies and speciation over all periods

Metals were analyzed in total, dissolved, and particulate forms in the influents and effluents during the *Normal*, *Dry*, and *Salt* periods. Over the whole experiment, the biochar beds significantly reduced the median total concentrations of most metals, including Co, Cr, Cu, Fe, Mn, and Pb ($p < 0.05$). In contrast, median total Cd and Ni concentrations were significantly higher in the effluent ($p < 0.05$), suggesting potential release from the biochar. The median total Zn concentration was also slightly elevated in the effluent, though not statistically significant ($p = 0.3$). In terms of metal speciation, all median particulate metal concentrations were significantly reduced ($p < 0.05$), except for Ni ($p = 0.3$), while dissolved median metal concentrations were consistently higher in the effluent than the influent ($p < 0.05$). These results indicate effective retention of particulate-bound metals, but also a shift toward the dissolved phase after particle separation. A similar pattern was reported by Lange et al. (2022) in Swedish highway stormwater, particularly for Cu, Pb, and Zn following bioretention treatment.

Some dissolved metal concentrations were consistently elevated in the effluent compared to the influent. For example, effluent dissolved Mn levels remained higher than the influent levels across all periods, likely due to its high solubility and sensitivity to redox conditions. Mn oxides readily reduce under saturated conditions and only precipitate effectively at pH values above 8 (Calugaru et al., 2018). To further explore where within the biochar beds metal mobilization occurred, additional samples were collected at 5, 50, and 95 cm from the inlet after each period (Fig. 3c). Dissolved concentrations of Co, Cu, Fe, Ni, and Pb generally increased with distance (See Supplementary Information Figure S5), especially after the *Dry* period. This suggests that metals were gradually released as water moved through the biochar bed. By 95 cm, concentrations often matched those in the effluent, indicating that

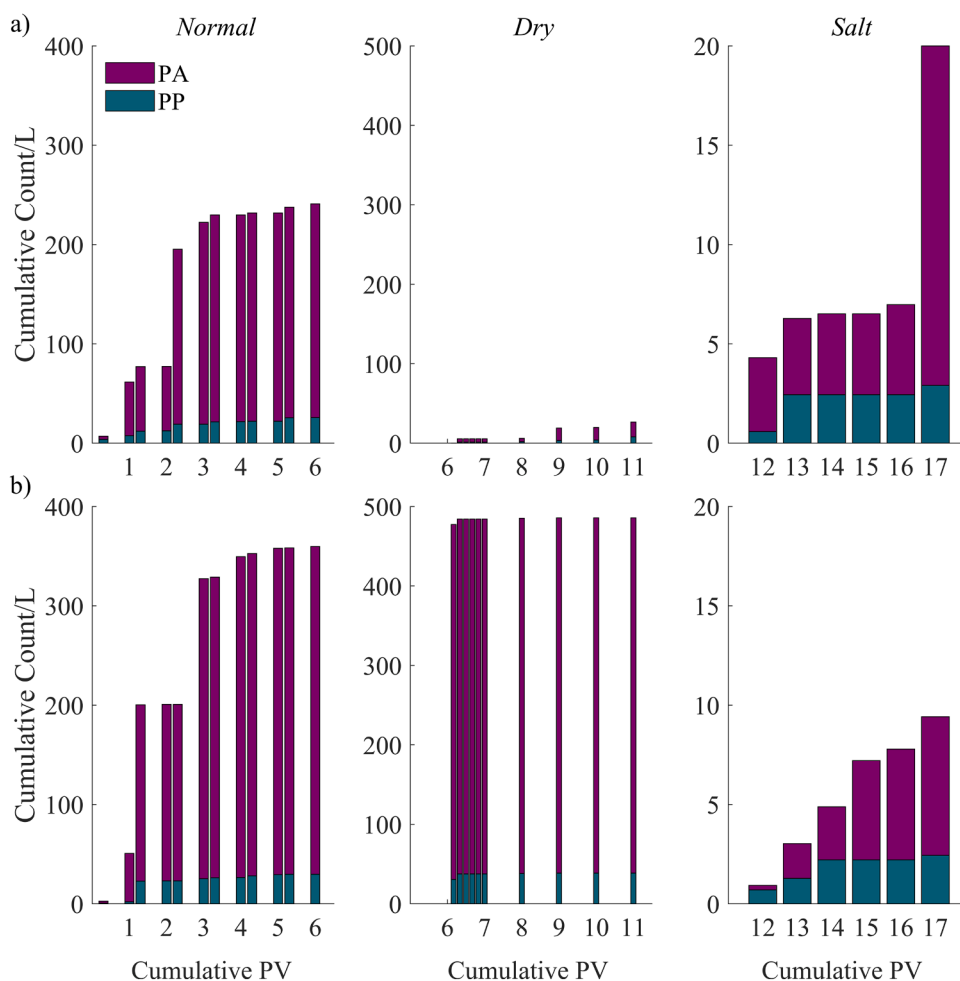


Fig. 7. Cumulative effluent PA and PP MP counts per L, for a) biochar bed F1 and b) biochar bed F2, over the periods *Normal*, *Dry*, and *Salt*, sampled at the cumulative pore volumes (PVs, x-axis) throughout the whole experiment.

Table 2

Median metal concentrations (µg/L) in influents and effluents over *Normal*, *Dry*, and *Salt* periods, including (Min, Max) values. The mean fraction of particulate-bound metals in influent semi-artificial stormwater over the periods is presented in percentage (%) with standard deviations. The total mass-based removal was calculated as $(Mass_{in} - Mass_{out}) / Mass_{in} \times 100$, compiled over each period.

	Cd	Co	Cr	Cu	Fe	Mn	Ni	Pb	Zn
Total metal concentrations over all periods									
Influent (µg/L):									
Median	0.04	2.4	20	13	10,000	260	2.7	4.0	110
Min	<LoQ	0.40	2.4	2.0	1900	35	0.20	0.60	12
Max	0.18	10	113	69	100,000	1200	16	14	400
Effluent (µg/L):									
Median	0.15	0.50	1.0	4.5	180	45	25	1.4	150
Min	0.020	0.030	0.30	1.1	3.8	7.6	<LoQ	0.10	17
Max	1.0	40	3.4	20	1100	280	150	6.0	880
Mean Fraction of Particulate-bound Metals (%) in Influent per period									
<i>Normal</i>	86	99	96	91	100	100	80	98	71
	±14	±0.70	±3.0	±5.0	±0.20	±0.30	±24	±1.9	±34
<i>Dry</i>	100	100	99	98	100	100	99	100	98
	±0.40	±0.10	±0.10	±0.30	±0.050	±0.10	±0.90	±0.10	±1.9
<i>Salt</i>	100	67	100	94	100	100	80	99	90
	±1.0	±78	±0.40	±7.0	±0.10	±0.040	±28	±1.2	±15
Mass-based Total Metal Removal (%) per period									
<i>Normal</i>	-20	92	96	75	99	91	-14	90	10
<i>Dry</i>	-450	61	95	73	97	33	-970	67	-140
<i>Salt</i>	-620	17	96	52	99	71	-800	63	-60

most mobilization occurred within the filter bed.

Effluent concentrations of dissolved and particulate metals, along with total event-based metal retention, are presented in Fig. 8,

illustrating changes across the different periods. During the *Normal* period (near-neutral pH; Fig. 4), total mass removal was high for Fe, Cr, Co, Mn, and Pb, while Cu was more variable with a mass-based removal

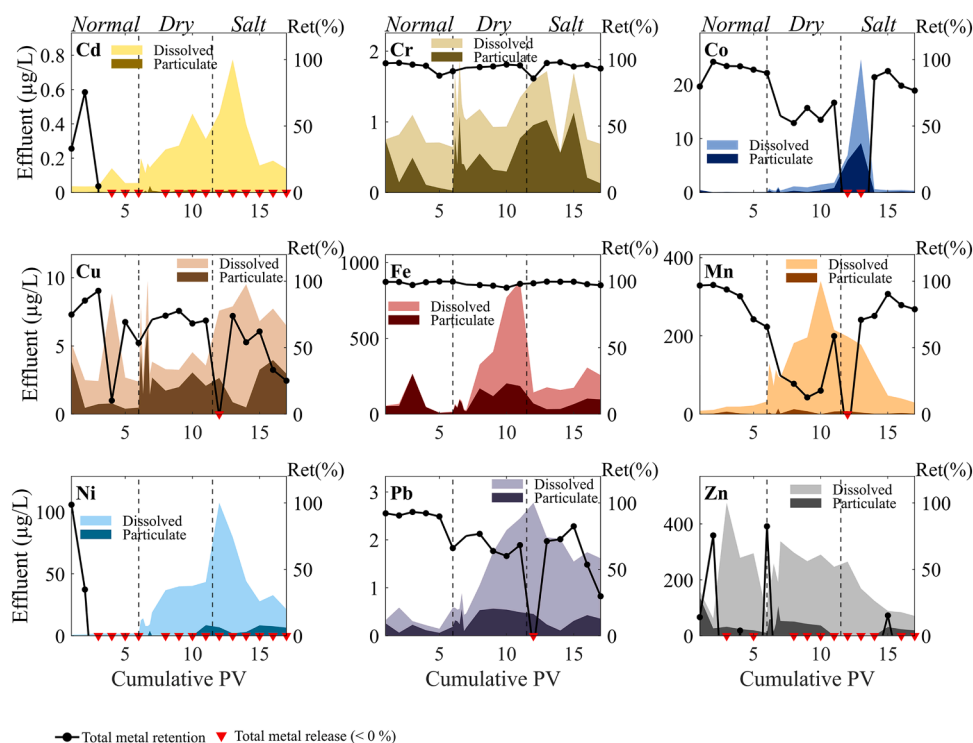


Fig. 8. Average dissolved and particulate metal concentrations in effluent from biochar beds F1 and F2 across each event in the *Normal*, *Dry*, and *Salt* periods. For each event, two effluent samples per replicate and event were analyzed for each total and dissolved metals; particulate concentrations were calculated as the difference (total – dissolved). Values represent the average across $n = 4$ effluent data points per event. Influent total metal concentrations were measured in triplicate per event, and their average was used to calculate event-based total metal retention (%) in the biochar beds (right y-axis, and black line). Red triangles indicate events with a net metal release. Event-based effluent metal concentrations are presented in the figures, while full datasets including measures of variability are provided in the Supplementary Information S10.

of 75 % (Table 2; Fig. 8). However, Zn exhibited a low mass reduction (10 %) during the *Normal* period, and Cd and Ni exhibited release from the substrate. These differences likely reflect metal speciation and pH sensitivity: at near-neutral pH, Cd, Ni, and Zn primarily occur as divalent cations that remain in solution (Esfandiar et al., 2022), and begin to form hydrolyzed species only above pH 7.7–8, limiting their ability to sorb to biochar surfaces (Davis and Leckie, 1978), whereas Cr, Co and Pb can form insoluble complexes at pH above 6 with organic matter or Fe/Mn-oxides (Moore et al., 1984).

During the *Dry* period when pH was more acidic (pH ~5; Fig. 4), total metal retention decreased for Mn, Co, and Pb, while Fe, Cr, and Cu remained largely unaffected (Table 2; Fig. 8). This reduced retention likely resulted from competition between H^+ ions and metal cations for sorption sites, as previously seen in stormwater treatment (Esfandiar and McKenzie, 2022), as well as the dissolution of Fe and Mn hydroxides at pH <6 (Eßer and Bassam, 1981). Iron and Mn hydroxide dissolution could have released previously attached metals such as Co^{2+} , Ni^{2+} , and Pb^{2+} (Fig. 8). In contrast, Cr retention remained high, likely due to its low solubility and tendency to hydrolyze at pH 4.5 and precipitate at pH 5.5, when in the +3 oxidation state (Griffin and Shimp, 1978). Additionally, Cu retention also remained stable, potentially due to strong complexation with organic matter, which remains effective even at pH as low as 5 (Zhao et al., 2024). Similar trends were reported by Sun et al. (2020), who found that wood-waste biochar removed a large fraction of total Cu, Cd, Ni, and Zn (80–100 %, 41–100 %, 44–84 %, and 51.6–100 %, respectively) at pH >6, while lower pH inhibited retention of all metals except Cu.

The *Salt* period introduced additional complexity, with increased salinity and pH fluctuations between 5.0–5.8 (Fig. 4). Mass removal of total Cr, Fe, and Pb remained comparable to the *Dry* period, while Cu removal declined to 52 %, and Co exhibited low removal (17 %; Table 2, Fig. 8). Decreased removal of metals with road-salt additions to

stormwater treatment filters has been noticed previously (Esfandiar and McKenzie, 2022). In this study, it is suggested that ion exchange was the primary mechanism of metal mobilization, as Co and Cu are more susceptible to displacement by Na^+ than metals like Pb and Zn (Schuler and Relyea, 2018). Similarly, Cr maintained stable retention under salinity stress, likely due to its limited susceptibility to ion exchange (Jolivet et al., 2004).

3.8. Potential co-transport of metals and microplastics

In this study, no statistically significant positive correlations were found between MP levels and metal concentrations. However, PA showed significant negative correlations with several metals ($\rho = -0.62$ to -0.51 , $p < 0.05$), including Mn, Ni, Cd, and Pb, while PP exhibited no significant correlations with any metals. These inverse relationships likely reflect experimental conditions in which MP retention increased over time (possibly due to filter clogging), whereas effluent metal concentrations increased following prolonged drying. Although interactions between MPs and dissolved metals may have occurred, their influence on system-level metal transport was likely limited by the relatively high biochar-to-MP mass ratio in the filters. As MPs were effectively retained within the biochar beds and their effluent concentrations decreased over time, any potential metal sorption to MPs would have had minimal opportunity to contribute to downstream transport. Instead, the observed increases in dissolved metal concentrations during the *Dry* and *Salt* periods are more consistently explained by pH-driven desorption and ion-exchange processes rather than by MP co-transport.

Overall, within the conditions tested in this study, no evidence was found to support MPs acting as a significant vector for metal transport. This outcome is likely influenced by the dominance of the filter media relative to MP mass. As such, while co-transport cannot be rejected in a general sense, it is not supported by the present findings. Nevertheless,

interactions between MPs and metals remain environmentally relevant, given the demonstrated role of MPs as vectors for pollutants (Liu et al., 2022), and the influence of MP surface properties, such as polarity, on metal sorption (Yang et al., 2019). Continued research is therefore needed to assess under which environmental conditions MPs may contribute more substantially to metal mobility, as suggested by Guan et al. (2020).

3.9. Treatment performance of biochar beds

The introduction of stressors such as prolonged drying and road salt application influenced the performance of the biochar beds. In this study, prolonged drying was associated with the release of previously retained particles, including MPs, consistent with colloid release observed during wet and dry cycles (Borthakur et al., 2021). Similar responses have been reported in bioretention systems, where prolonged drying reduces treatment performance by promoting the oxidation of organic matter, leading to pH decline, and inducing physical changes in the media, such as preferential flow path formation and media washout (Blecken et al., 2009; Lange et al., 2020). The biochar beds showed limited capacity to buffer the pH decline in the *Dry* and *Salt* periods, which raises concern, as effluent acidification can enhance material corrosion, degrade water quality (Kuang and Sansalone, 2011), and increase metal solubility (Bradl, 2004), thereby elevating the risk of metal toxicity in receiving waters. This pH decrease, along with the addition of road salt, was reflected in the mobilization of metals, with elevated dissolved effluent concentrations, some of which exceeded environmental quality standards. According to site-specific thresholds from Swedish water quality guidance (Vattenmyndigheten, 2019), Pb and Cu levels remained below or near the guideline values, while Ni concentrations exceeded the 16 µg/L threshold, indicating site-specific pollution and potential ecological risk. In contrast to previous field and column studies that report particle dispersion under sodic conditions (Flanagan et al., 2019), no turbidity increase was observed during the *Salt* period. This discrepancy may be attributed to the particulate composition in this system, which is dominated by road dust rather than native soils.

4. Conclusion

This study demonstrates the potential of biochar beds to effectively remove both MPs and particulate-bound metals from stormwater, providing valuable insights for urban stormwater management. Results indicate that MP removal followed polymer- and size-dependent patterns, with non-polar PP fragments retained more efficiently than polar PA, especially during early filter operation. Environmental stressors are believed to have influenced MP behavior, where prolonged drying led to a pulse release of MPs. At the same time, acidic and saline conditions may have enhanced PA sorption through altered electrostatic interactions with the biochar. Under *Normal*, near-neutral conditions, biochar effectively retained most metals. However, leaching of metals such as Cd and Ni from the biochar was observed and biochar bed performance was sensitive to environmental changes such as acidification during *Dry* periods and increased salinity during the *Salt* period. These conditions promoted metal desorption, shifted metal speciation toward more mobile dissolved forms, and reduced adsorption efficiency through ion competition. While metals like Cr and Fe were consistently retained, others displayed complex, episode-dependent behavior, highlighting the need to design filter systems that accommodate seasonal and chemical variability in stormwater inputs. No direct correlation between the release of MPs and metals was found in this study. However, co-transport remains a relevant concern, as MPs can influence the fate and mobility of other pollutants. Taken together, these findings highlight the importance of evaluating filter systems under realistic and stress-prone scenarios. Future research should further investigate how environmental variability affects the co-removal of MPs and metals in

biochar-based filters, and guide the development of filter designs that maintain robust performance across diverse stormwater conditions.

Funding sources

This work is part of the project “Cities with Less Microplastics: Roadside Green Filters to Remove Microplastics from Urban Stormwater,” funded by the Swedish Research Council for Environment, Agricultural Sciences and Spatial Planning (FORMAS), grant number 2019–01,911.

Acknowledgements declaration of generative AI and AI-assisted technologies in the writing process

During the preparation of this work the authors used CHATGPT-4 in proof-reading and improving the grammar of the manuscript. After using this tool, the authors reviewed and edited the content as needed and takes full responsibility for the content of the publication.

CRedit authorship contribution statement

Gabriella Rullander: Writing – review & editing, Writing – original draft, Visualization, Validation, Software, Project administration, Methodology, Investigation, Formal analysis, Data curation, Conceptualization. **Roger Herbert:** Writing – review & editing, Visualization, Validation, Supervision, Resources, Project administration, Methodology, Formal analysis, Conceptualization. **Ann-Margret Strömvall:** Writing – review & editing, Visualization, Validation, Supervision, Resources, Project administration, Methodology, Formal analysis, Conceptualization. **Jes Vollertsen:** Writing – review & editing, Visualization, Validation, Supervision, Software, Resources, Project administration, Methodology, Formal analysis, Conceptualization. **Claudia Lorenz:** Writing – review & editing, Visualization, Validation, Supervision, Project administration, Methodology, Formal analysis, Conceptualization. **Sebastien Rauch:** Writing – review & editing, Visualization, Validation, Resources, Project administration, Methodology, Investigation, Formal analysis, Data curation, Conceptualization. **Amir Saeid Mohammadi:** Writing – review & editing, Visualization, Validation, Resources, Project administration, Methodology, Investigation, Formal analysis, Data curation, Conceptualization. **Sahar S. Dalahmeh:** Writing – review & editing, Visualization, Validation, Supervision, Resources, Project administration, Methodology, Funding acquisition, Formal analysis, Conceptualization.

Declaration of competing interest

The authors declare that they have no known competing financial or personal interests that could have influenced the work reported in this paper.

Acknowledgements

We thank the Campus Management Unit Lagerrådet at the Department of Earth Sciences, Uppsala University, for their support in transporting and implementing the biochar beds. We also appreciate the additional efforts and metal analyses conducted at the laboratory of Chalmers University of Technology, and we are thankful to Dr. Lucian Iordachescu for his expert assistant in analyzing microplastic control samples at Aalborg University.

Supplementary materials

Supplementary material associated with this article can be found, in the online version, at [doi:10.1016/j.envc.2026.101407](https://doi.org/10.1016/j.envc.2026.101407).

Data availability

Data will be made available on request.

References

- Ahmad, M., Lubis, N.M.A., Usama, M., Ahmad, J., Al-Wabel, M.I., Al-Swadi, H.A., Rafique, M.I., Al-Farraj, A.S.F., 2023. Scavenging microplastics and heavy metals from water using jujube waste-derived biochar in fixed-bed column trials. *Environ. Pollut.* 335, 122319. <https://doi.org/10.1016/j.envpol.2023.122319>.
- Antonson, H., Buckland, P., Blomqvist, G., 2021. Road salt damage to historical milestones indicates adaptation of winter roads to future climate change may damage Arctic cultural heritage. *Climate* 9, 149. <https://doi.org/10.3390/cli9100149>.
- Bashir, M., Mohan, C., Tyagi, S., Annachatre, A., 2022. Copper removal from aqueous solution using chemical precipitation and adsorption by Himalayan Pine Forest Residue as Biochar. *Water. Sci. Technol.* 86, 530–554. <https://doi.org/10.2166/wst.2022.222>.
- Björklund, K., Cousins, A.P., Strömwall, A.-M., Malmqvist, P.-A., 2009. Phthalates and nonylphenols in urban runoff: occurrence, distribution and area emission factors. *Sci. Total. Environ.* 407, 4665–4672. <https://doi.org/10.1016/j.scitotenv.2009.04.040>.
- Blecken, G.-T., Zinger, Y., Deletić, A., Fletcher, T.D., Viklander, M., 2009. Influence of intermittent wetting and drying conditions on heavy metal removal by stormwater biofilters. *Water. Res.* 43, 4590–4598. <https://doi.org/10.1016/j.watres.2009.07.008>.
- Borthakur, A., Olsen, P., Dooley, G., Cranmer, B., Rao, U., Hoek, E., Blotvogel, J., Mahendra, S., Mohanty, S., 2021. Dry-wet and freeze-thaw cycles enhance PFOA leaching from subsurface soils. *J. Hazard. Mater. Lett.* 2, 100029. <https://doi.org/10.1016/j.hazl.2021.100029>.
- Brad, H.B., 2004. Adsorption of heavy metal ions on soils and soils constituents. *J. Colloid. Interface Sci.* 277, 1–18. <https://doi.org/10.1016/j.jcis.2004.04.005>.
- Calugaru, I.L., Neculita, C.M., Genty, T., Zagury, G.J., 2018. Metals and metalloids treatment in contaminated neutral effluents using modified materials. *J. Environ. Manag.* 212, 142–159. <https://doi.org/10.1016/j.jenvman.2018.02.002>.
- Campanale, C., Massarelli, C., Savino, I., Locaputo, V., Uricchio, V.F., 2020. A detailed review study on potential effects of microplastics and additives of concern on Human health. *Int. J. Environ. Res. Public Health* 17. <https://doi.org/10.3390/ijerph17041212>.
- Chen, W.-H., Hoang, A.T., Nizetić, S., Pandey, A., Cheng, C.K., Luque, R., Ong, H.C., Thomas, S., Nguyen, X.P., 2022. Biomass-derived biochar: from production to application in removing heavy metal-contaminated water. *Process. Saf. Environ. Prot.* 160, 704–733. <https://doi.org/10.1016/j.psep.2022.02.061>.
- Davis, J.A., Leckie, J.O., 1978. Effect of adsorbed complexing ligands on trace metal uptake by hydrous oxides. *Environ. Sci. Technol.* 12, 1309–1315. <https://doi.org/10.1021/es60147a006>.
- Davis, A.P., 2005. Green engineering principles promote low-impact development. *Environ. Sci. Technol.* 39, 339A–344A.
- Eßer, J., Bassam, N.E., 1981. On the mobility of cadmium under aerobic soil conditions. *Environ. Pollut. Ser. Ecol. Biol.* 26, 15–31.
- Ekvall, J., Strand, M., 2001. *Dagvattenundersökningar i Stockholm 1992–2000*. Stockholm Vatten och Avfall, Stockholm.
- Eriksson, E., Baun, A., Scholes, L., Ledin, A., Ahlman, S., Revitt, M., Noutsopoulos, C., Mikkelsen, P.S., 2007. Selected stormwater priority pollutants — A European perspective. *Sci. Total. Environ.* 383, 41–51. <https://doi.org/10.1016/j.scitotenv.2007.05.028>.
- Esfandiar, N., McKenzie, E.R., 2022. Bioretention soil capacity for removing nutrients, metals, and polycyclic aromatic hydrocarbons: roles of co-contaminants, pH, salinity and dissolved organic carbon. *J. Environ. Manage.* 324, 116314. <https://doi.org/10.1016/j.jenvman.2022.116314>.
- Esfandiar, N., Suri, R., McKenzie, E.R., 2022. Competitive sorption of Cd, Cr, Cu, Ni, Pb and Zn from stormwater runoff by five low-cost sorbents; effects of co-contaminants, humic acid, salinity and pH. *J. Hazard. Mater.* 423, 126938. <https://doi.org/10.1016/j.jhazmat.2021.126938>.
- Flanagan, K., Branchu, P., Boudahmane, L., Caupos, E., Demare, D., Deshayes, S., Dubois, P., Meffray, L., Partibane, C., Saad, M., Gromaire, M.-C., 2018. Field performance of two biofiltration systems treating micropollutants from road runoff. *Water. Res.* 145, 562–578. <https://doi.org/10.1016/j.watres.2018.08.064>.
- Flanagan, K., Branchu, P., Boudahmane, L., Caupos, E., Demare, D., Deshayes, S., Dubois, P., Meffray, L., Partibane, C., Saad, M., 2019. Retention and transport processes of particulate and dissolved micropollutants in stormwater biofilters treating road runoff. *Sci. Total. Environ.* 656, 1178–1190.
- Göbel, P., Dierkes, C., Coldewey, W.G., 2007. Storm water runoff concentration matrix for urban areas. *J. Contam. Hydrol.* 91, 26–42. <https://doi.org/10.1016/j.jconhyd.2006.08.008>.
- Gaggini, E.L., Polukarova, M., Bondelind, M., Rödland, E., Strömwall, A.-M., Andersson-Sköld, Y., Sokolova, E., 2024. Assessment of fine and coarse tyre wear particles along a highway stormwater system and in receiving waters: occurrence and transport. *J. Environ. Manag.* 367, 121989. <https://doi.org/10.1016/j.jenvman.2024.121989>.
- Ghavanloughajari, M., Valencia, R., Le, H., Rahman, M., Borthakur, A., Ravi, S., Stenstrom, M.K., Mohanty, S.K., 2020. Compaction conditions affect the capacity of biochar-amended sand filters to treat road runoff. *Sci. Total. Environ.* 735, 139180. <https://doi.org/10.1016/j.scitotenv.2020.139180>.
- Griffin, R.A., Shimp, N.F., 1978. Attenuation of Pollutants in Municipal Landfill Leachate by Clay Minerals. U.S. EPA, United States. <https://www.osti.gov/biblio/6312927>.
- Guan, J., Qi, K., Wang, J., Wang, W., Wang, Z., Lu, N., Qu, J., 2020. Microplastics as an emerging anthropogenic vector of trace metals in freshwater: significance of biofilms and comparison with natural substrates. *Water. Res.* 184, 116205. <https://doi.org/10.1016/j.watres.2020.116205>.
- Hunt, W.F., Davis, A.P., Traver, R.G., 2012. Meeting hydrologic and water quality goals through targeted bioretention design. *J. Environ. Eng.* 138, 698–707. [https://doi.org/10.1061/\(ASCE\)EE.1943-7870.0000504](https://doi.org/10.1061/(ASCE)EE.1943-7870.0000504).
- Iordachescu, L., Rullander, G., Lykkemark, J., Dalahmeh, S., Vollertsen, J., 2024. An integrative analysis of microplastics in spider webs and road dust in an urban environment—webbed routes and asphalt trails. *J. Environ. Manag.* 359, 121064. <https://doi.org/10.1016/j.jenvman.2024.121064>.
- Ivleva, N.P., 2021. Chemical analysis of microplastics and nanoplastics: challenges, advanced methods, and perspectives. *Chem. Rev.* 121, 11886–11936. <https://doi.org/10.1021/acs.chemrev.1c00178>.
- Järllskog, I., Strömwall, A.-M., Magnusson, K., Gustafsson, M., Polukarova, M., Galfi, H., Aronsson, M., Andersson-Sköld, Y., 2020. Occurrence of tire and bitumen wear microplastics on urban streets and in sweepsand and washwater. *Sci. Total. Environ.* 729, 138950. <https://doi.org/10.1016/j.scitotenv.2020.138950>.
- Järllskog, I., Strömwall, A.-M., Magnusson, K., Galfi, H., Björklund, K., Polukarova, M., Garção, R., Markiewicz, A., Aronsson, M., Gustafsson, M., Norin, M., Blom, L., Andersson-Sköld, Y., 2021. Traffic-related microplastic particles, metals, and organic pollutants in an urban area under reconstruction. *Sci. Total. Environ.* 774, 145503. <https://doi.org/10.1016/j.scitotenv.2021.145503>.
- Johansson, G., Fedje, K.K., Modin, O., Haeger-Eugensson, M., Uhl, W., Andersson-Sköld, Y., Strömwall, A.-M., 2024. Removal and release of microplastics and other environmental pollutants during the start-up of bioretention filters treating stormwater. *J. Hazard. Mater.* 468, 133532. <https://doi.org/10.1016/j.jhazmat.2024.133532>.
- Johansson, G., Polukarova, M., Fedje, K.K., Modin, O., Andersson-Sköld, Y., Strömwall, A.-M., 2025. Removal of microplastics, organic pollutants and metals from stormwater in bioretention filters with added sorbent material during simulated extreme rainfall events under winter conditions with dormant plants. *J. Hazard. Mater.* 496, 138868. <https://doi.org/10.1016/j.jhazmat.2025.138868>.
- Jolivet, J.-P., Chanéac, C., Tronc, E., 2004. Iron oxide chemistry. From molecular clusters to extended solid networks. *Chem. Commun. Camb. Engl.* 35, 481–487. <https://doi.org/10.1039/b304532n>.
- Kuang, X., Sansalone, J., 2011. Cementitious porous pavement in stormwater quality control: pH and alkalinity elevation. *Water. Sci. Technol.* 63, 2992–2998. <https://doi.org/10.2166/wst.2011.505>.
- Lange, K., Viklander, M., Blecken, G.-T., 2020. Effects of plant species and traits on metal treatment and phytoextraction in stormwater bioretention. *J. Environ. Manag.* 276, 111282. <https://doi.org/10.1016/j.jenvman.2020.111282>.
- Lange, K., Magnusson, K., Viklander, M., Blecken, G.-T., 2021. Removal of rubber, bitumen and other microplastic particles from stormwater by a gross pollutant trap - bioretention treatment train. *Water. Res.* 202, 117457. <https://doi.org/10.1016/j.watres.2021.117457>.
- Lange, K., Osterlund, H., Viklander, M., Blecken, G.-T., 2022a. Occurrence and concentration of 20–100 µm sized microplastic in highway runoff and its removal in a gross pollutant trap – Bioretention and sand filter stormwater treatment train. *Sci. Total. Environ.* 809, 151151. <https://doi.org/10.1016/j.scitotenv.2021.151151>.
- Lange, K., Viklander, M., Blecken, G.-T., 2022b. Investigation of intra - event variations of total, dissolved and truly dissolved metal concentrations in highway runoff and a gross pollutant trap – bioretention stormwater treatment train. *Water. Res.* 216, 118284. <https://doi.org/10.1016/j.watres.2022.118284>.
- Liu, S., Shi, J., Wang, J., Dai, Y., Li, H., Li, J., Liu, X., Chen, X., Wang, Z., Zhang, P., 2021. Interactions between microplastics and heavy metals in aquatic environments: a review. *Front. Microbiol.* 12. <https://doi.org/10.3389/fmicb.2021.652520>.
- Liu, S., Huang, J., Zhang, W., Shi, L., Yi, K., Yu, H., Zhang, C., Li, S., Li, J., 2022. Microplastics as a vehicle of heavy metals in aquatic environments: a review of adsorption factors, mechanisms, and biological effects. *J. Environ. Manag.* 302, 113995. <https://doi.org/10.1016/j.jenvman.2021.113995>.
- Müller, A., Österlund, H., Marsalek, J., Viklander, M., 2020. The pollution conveyed by urban runoff: a review of sources. *Sci. Total. Environ.* 709, 136125. <https://doi.org/10.1016/j.scitotenv.2019.136125>.
- Markiewicz, A., Björklund, K., Eriksson, E., Kalmykova, Y., Strömwall, A.-M., Siopi, A., 2017. Emissions of organic pollutants from traffic and roads: priority pollutants selection and substance flow analysis. *Sci. Total. Environ.* 580, 1162–1174. <https://doi.org/10.1016/j.scitotenv.2016.12.074>.
- Marsalek, J., 2003. Road salts in urban stormwater: an emerging issue in stormwater management in cold climates. *Water. Sci. Technol.* 48, 61–70. <https://doi.org/10.2166/wst.2003.0493>.
- Monira, S., Bhuiyan, M.A., Haque, N., Shah, K., Roychand, R., Hai, F.I., Pramanik, B.K., 2021. Understanding the fate and control of road dust-associated microplastics in stormwater. *Process. Saf. Environ. Prot.* 152, 47–57. <https://doi.org/10.1016/j.psep.2021.05.033>.
- Moore, J.W., Ramamoorthy, S., Ballantyne, E.E., 1984. *Heavy Metals in Natural waters: Applied Monitoring and Impact Assessment*. Springer-Verlag, New York.
- Mota, L.S.O., de Oliveira, P.C.O., Peixoto, B.S., Bezerra, E.S., de Moraes, M.C., 2025. Biochar applications in microplastic and nanoplastic removal: mechanisms and integrated approaches. *Environ. Sci. Water Res. Technol.* 11, 222–241. <https://doi.org/10.1039/d4ew00709c>.
- Mukherjee, A., Zimmerman, A.R., 2013. Organic carbon and nutrient release from a range of laboratory-produced biochars and biochar-soil mixtures. *Geoderma* 193–194, 122–130. <https://doi.org/10.1016/j.geoderma.2012.10.002>.

- Novotny, V., Muehring, D., Zitomer, D.H., Smith, D.W., Facey, R., 1998. Cyanide and metal pollution by urban snowmelt: impact of deicing compounds. *Water. Sci. Technol.* 38, 223–230. [https://doi.org/10.1016/s0273-1223\(98\)00753-7](https://doi.org/10.1016/s0273-1223(98)00753-7).
- Paul, D., Kaser, N., Kolar, P., Hall, S.G., 2020. Physicochemical characterization data of pine-derived biochar and natural zeolite as precursors to catalysts. *Chem. Data Collect.* 30, 100573. <https://doi.org/10.1016/j.cdc.2020.100573>.
- Paus, K., Morgan, J., Gulliver, J., Leiknes, T., Hozalski, R., 2014. Effects of temperature and NaCl on toxic metal retention in bioretention Media. *J. Environ. Eng.* 140. [https://doi.org/10.1061/\(ASCE\)EE.1943-7870.0000847](https://doi.org/10.1061/(ASCE)EE.1943-7870.0000847).
- Primpke, S., Cross, R.K., Mintenig, S.M., Simon, M., Vianello, A., Gerdts, G., Vollertsen, J., 2020. Toward the systematic identification of microplastics in the environment: evaluation of a new independent software tool (siMPle) for spectroscopic analysis. *Appl. Spectrosc.* 74, 1127–1138. <https://doi.org/10.1177/0003702820917760>.
- Robinson, H.K., Hasenmueller, E.A., 2017. Transport of road salt contamination in karst aquifers and soils over multiple timescales. *Sci. Total. Environ.* 603–604, 94–108. <https://doi.org/10.1016/j.scitotenv.2017.05.244>.
- Rosso, B., Corami, F., Vezzaro, L., Biondi, S., Bravo, B., Barbante, C., Gambaro, A., 2022. Quantification and characterization of additives, plasticizers, and small microplastics (5–100 µm) in highway stormwater runoff. *J. Environ. Manag.* 324, 116348. <https://doi.org/10.1016/j.jenvman.2022.116348>.
- Rullander, G., Lorenz, C., Strömval, A.-M., Vollertsen, J., Dalahmeh, S.S., 2024. Bark and biochar in horizontal flow filters effectively remove microplastics from stormwater. *Environ. Pollut.* 356, 124335. <https://doi.org/10.1016/j.envpol.2024.124335>.
- Saget, A., Chebbo, G., Bertrand-Krajewski, J.-L., 1996. The first flush in sewer systems. *Water. Sci. Technol.* 33, 101–108. [https://doi.org/10.1016/0273-1223\(96\)00375-7](https://doi.org/10.1016/0273-1223(96)00375-7).
- Schelde, K., Moldrup, P., Jacobsen, O.H., de Jonge, H., de Jonge, L.W., Komatsu, T., 2002. Diffusion-limited mobilization and transport of natural colloids in macroporous soil. *Vadose Zone J.* 1, 125–136. <https://doi.org/10.2113/1.1.125>.
- Schuler, M.S., Relyea, R.A., 2018. A review of the combined threats of road salts and heavy metals to freshwater systems. *Bioscience* 68, 327–335. <https://doi.org/10.1093/biosci/biy018>.
- Shafi, M., Lodh, A., Khajuria, M., Ranjan, V.P., Gani, K.M., Chowdhury, S., Goel, S., 2024. Are we underestimating stormwater? Stormwater as a significant source of microplastics in surface waters. *J. Hazard. Mater.* 465, 133445. <https://doi.org/10.1016/j.jhazmat.2024.133445>.
- Shetty, N.H., Mailloux, B.J., McGillis, W.R., Culligan, P.J., 2020. Observations of the seasonal buildup and washout of salts in urban bioswale soil. *Sci. Total. Environ.* 722, 137834. <https://doi.org/10.1016/j.scitotenv.2020.137834>.
- Sjökvist, E., Asp, M., Mårtensson, J.A., Berggreen-Clausen, S., Berglöv, G., Björck, E., Nylén, L., Ohlsson, A., Persson, H., 2015. Framtidsklimat i Uppsala län - enligt RCP-scenarier. SMHI, Norrköping.
- Smyth, K., Drake, J., Li, Y., Rochman, C., Van Seters, T., Passeport, E., 2021. Bioretention cells remove microplastics from urban stormwater. *Water. Res.* 191, 116785. <https://doi.org/10.1016/j.watres.2020.116785>.
- Sun, Y., Chen, S.S., Lau, A.Y.T., Tsang, D.C.W., Mohanty, S.K., Bhatnagar, A., Rinklebe, J., Lin, K.-Y.A., Ok, Y.S., 2020. Waste-derived compost and biochar amendments for stormwater treatment in bioretention column: co-transport of metals and colloids. *J. Hazard. Mater.* 383, 121243. <https://doi.org/10.1016/j.jhazmat.2019.121243>.
- Tan, X., Liu, Y., Zeng, G., Wang, X., Hu, X., Gu, Y., Yang, Z., 2015. Application of biochar for the removal of pollutants from aqueous solutions. *Chemosphere* 125, 70–85. <https://doi.org/10.1016/j.chemosphere.2014.12.058>.
- Tong, M., He, L., Rong, H., Li, M., Kim, H., 2020. Transport behaviors of plastic particles in saturated quartz sand without and with biochar/Fe3O4-biochar amendment. *Water. Res.* 169, 115284. <https://doi.org/10.1016/j.watres.2019.115284>.
- Valizadeh, S., Lee, S.S., Choi, Y.J., Baek, K., Jeon, B.-H., Lin, K.-Y.A., Park, Y.-K., 2022. Biochar application strategies for polycyclic aromatic hydrocarbons removal from soils. *Environ. Res.* 213, 113599. <https://doi.org/10.1016/j.envres.2022.113599>.
- Vattenmyndigheten, H., 2019. Havs-och vattenmyndighetens föreskrifter om klassificering och miljö kvalitetsnormer avseende ytvattnet. HVMFS 25, 88.
- Vianello, A., Jensen, R.L., Liu, L., Vollertsen, J., 2019. Simulating human exposure to indoor airborne microplastics using a breathing thermal Manikin. *Sci. Rep.* 9, 8670. <https://doi.org/10.1038/s41598-019-45054-w>.
- Vieira, Y., Lima, E.C., Foletto, E.L., Dotto, G.L., 2021. Microplastics physicochemical properties, specific adsorption modeling and their interaction with pharmaceuticals and other emerging contaminants. *Sci. Total. Environ.* 753, 141981. <https://doi.org/10.1016/j.scitotenv.2020.141981>.
- Vijayan, A., Österlund, H., Magnusson, K., Marsalek, J., Viklander, M., 2022. Microplastics (MPs) in urban roadside snowbanks: quantities, size fractions and dynamics of release. *Sci. Total. Environ.* 851, 158306. <https://doi.org/10.1016/j.scitotenv.2022.158306>.
- Wang, Z., Sedighi, M., Lea-Langton, A., 2020. Filtration of microplastic spheres by biochar: removal efficiency and immobilisation mechanisms. *Water. Res.* 184, 116165. <https://doi.org/10.1016/j.watres.2020.116165>.
- Yaashikaa, P.R., Kumar, P.S., Varjani, S., Saravanan, A., 2020. A critical review on the biochar production techniques, characterization, stability and applications for circular bioeconomy. *Biotechnol. Rep.* 28, e00570. <https://doi.org/10.1016/j.btre.2020.e00570>.
- Yang, J., Cang, L., Sun, Q., Dong, G., Ata-Ul-Karim, S.T., Zhou, D., 2019. Effects of soil environmental factors and UV aging on Cu2+ adsorption on microplastics. *Environ. Sci. Pollut. Res.* 26, 23027–23036. <https://doi.org/10.1007/s11356-019-05643-8>.
- Youngwilai, A., Phungsai, P., Supanchaiyamat, N., Hunt, A.J., Ngernyen, Y., Ratpukdi, T., Khan, E., Siripattanakul-Ratpukdi, S., 2022. Characterization of dissolved organic carbon and disinfection by-products in biochar filter leachate using orbitrap mass spectrometry. *J. Hazard. Mater.* 424, 127691. <https://doi.org/10.1016/j.jhazmat.2021.127691>.
- Zgheib, S., Moillon, R., Chebbo, G., 2012. Priority pollutants in urban stormwater: part 1 – Case of separate storm sewers. *Water. Res.* 46, 6683–6692. <https://doi.org/10.1016/j.watres.2011.12.012>.
- Zhao, S., Zhao, Y., Cui, Z., Zhang, H., Zhang, J., 2024. Effect of pH, temperature, and salinity levels on heavy metal fraction in lake sediments. *Toxics* 12, 494. <https://doi.org/10.3390/toxics12070494>.